REFRACTT 2006

Real-Time Retrieval of High-Resolution, Low-Level Moisture Fields from Operational NEXRAD and Research Radars

BY RITA D. ROBERTS, FRÉDÉRIC FABRY, PATRICK C. KENNEDY, ERIC NELSON, JAMES W. WILSON, NANCY REHAK, JASON FRITZ, V. CHANDRASEKAR, JOHN BRAUN, JUANZHEN SUN, SCOTT ELLIS, STEVEN REISING, TIMOTHY CRUM, LARRY MOONEY, ROBERT PALMER, TAMMY WECKWERTH, AND SHARMILA PADMANABHAN

High-resolution moisture fields retrieved for the first time from both operational and research radars illustrate the low-level moisture variability associated with boundary layer processes and the prethunderstorm environment.

Several national study groups (National Research Council 1998; Emanuel et al. 1995; Dabberdt and Schlatter 1996) have suggested that the lack of detailed, high-resolution water vapor measurements in the atmospheric boundary layer is one of the primary limiting factors in being able to predict the timing and location of convection initiation and to produce accurate quantitative precipitation forecasts (QPF). Humidity measurements from current operational surface station and radiosonde data provide discrete points of moisture information at 2–10 m AGL and ~250-m vertical resolution, respectively, but typically they are separated by distances of 10–100 km or greater. Moisture measurements can be retrieved over a higher spatial resolution from satellite data [e.g.; Moderate Resolution Imaging Spectroradiometer (MODIS) with 0.25–1-km resolution], but lack the high frequency of observations that are needed for the short-term forecasting of thunderstorms. Accurate measurements of moisture variability over high spatial and temporal resolution are needed for improvement in QPF and to forecast the onset of convection, which has shown to be thermodynamically sensitive to moisture and temperature perturbations in the boundary layer of only 1 g kg^{-1} and 1°C, respectively (Crook 1996).

AFFILIATIONS: ROBERTS, NELSON, WILSON, REHAK, SUN, ELLIS, AND WECKWERTH—National Center for Atmospheric Research, Boulder, Colorado; FABRY—McGill University, Montreal, Quebec, Canada; KENNEDY, FRITZ, CHANDRASEKAR, REISING, AND PADMANABHAN—Colorado State University, Fort Collins, Colorado; CRUM—Radar Operations Center, NOAA/National Weather Service, Norman, Oklahoma; BRAUN—University Corporation for Atmospheric Research, COSMIC, Boulder, Colorado; MOONEY—Denver Forecast Office, National Weather Service, Boulder, Colorado; PALMER—University of Oklahoma, Norman, Oklahoma

CORRESPONDING AUTHOR: Rita D. Roberts, National Center for Atmospheric Research, 3450 Mitchell Lane, Boulder, CO 80301
E-mail: rroberts@ucar.edu

The abstract for this article can be found in this issue, following the table of contents.
DOI:10.1175/2008BAMS2412.1

In final form 15 April 2008

One of the most promising outcomes of the International H_2O Project (IHOP_2002; Weckwerth et al. 2004), conducted in 2002, was the near-surface, high-resolution water vapor measurements extracted from radar using an index of refraction (refractivity) technique developed by Fabry et al. (1997). This technique is based on the concept that variability in the received phase of radar waves propagating between the radar and fixed ground targets (such as buildings, radio towers, silos) is due to changes in the properties of air (i.e., changes in index of refraction) between the radar and the targets. In essence, the presence of water vapor in the atmosphere changes the speed at which the radar waves travel through the air between the radar and fixed ground objects. By applying this novel refractivity approach to the remote sensing of ground targets by radar, it is now possible to retrieve moisture estimates in the near-surface boundary layer to high spatial (4 km) and temporal (4 min) resolution. *Radar measurements of refractivity give us an exciting new glimpse of the mesoscale variability of moisture in the same manner in which measurements of radar reflectivity gave us our first view of the mesoscale structure of precipitation half a century ago (Fabry 2006).*

The Refractivity Experiment for H_2O Research and Collaborative Operational Technology Transfer (REFRACTT), conducted from June to August 2006 in northeastern Colorado, provided an ideal opportunity to demonstrate the value of this high-resolution 2D moisture field to the research and operational community through the collection of refractivity data over a multiradar domain that included a Next Generation Weather Radar (NEXRAD) and three research radars, all of which are 10-cm-wavelength (S band) radars. The major outcome of REFRACTT 2006 was the collection of moisture information over a several-hundred-kilometer domain, which is rich in detail, for exploring subtleties in the movement of water vapor through the atmosphere. The benefit of REFRACTT is the opportunity to improve our understanding of water vapor variability and the role it plays in the initiation of convection and thunderstorms. We envision that these enhanced observations will lead to increased accuracy in quantitative precipitation forecasts through assimilation of the moisture fields into mesoscale numerical models. Of great interest operationally, REFRACTT 2006 successfully demonstrated that accurate moisture information could be retrieved from NEXRAD without interference to normal operations, which opens up the realm of moisture sensing possibilities if this technique is installed on the national network of operational radars.

Figure 1 shows the REFRACTT domain and the radar locations. The 50-km-range rings represent the typical extent for which the radars will detect reliable return signals from fixed ground targets. The locations of the radars were fortuitous because the overlapping

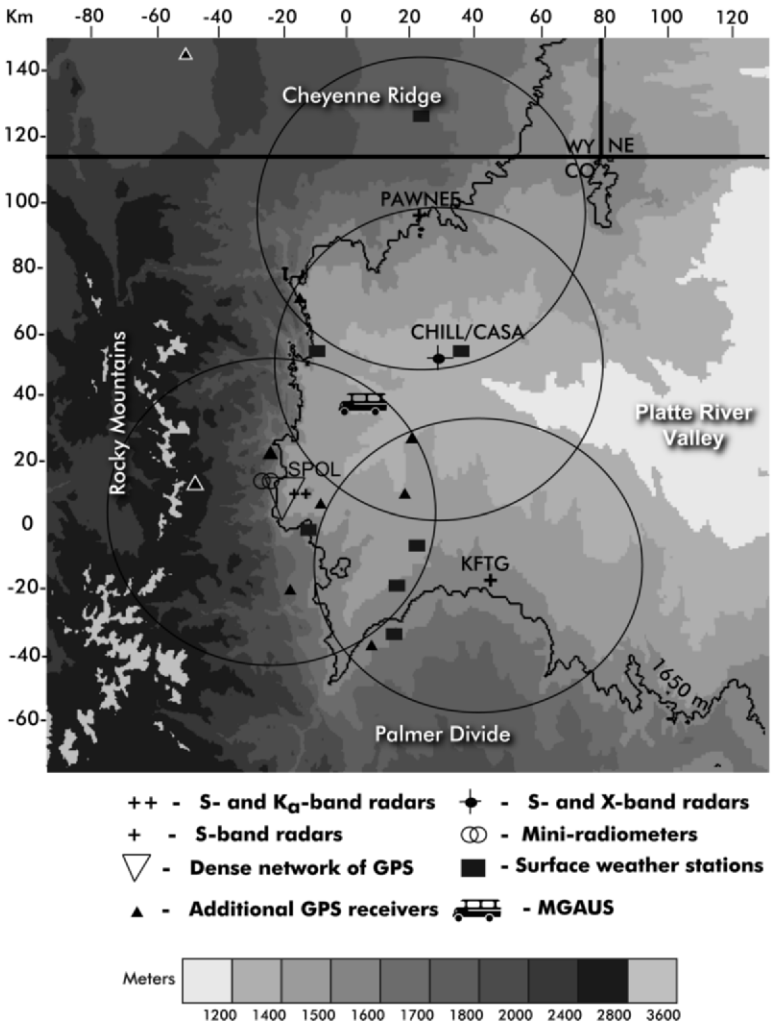

Fig. 1. The REFRACTT domain overlaid onto the topography of northeast Colorado. Locations of the deployed instrumentation are shown. Highlighted in black is the terrain contour for the 1,650-m elevation. The 50-km ring surrounding each radar represents the typical range for which the radars will detect reliable ground targets.

observations of targets facilitated comparison of moisture estimates from two or more radars and provided a unique opportunity to mosaic the refractivity fields together to observe moisture variability and transport over a much larger domain. Additional moisture retrieval instrumentation fielded during REFRACTT 2006 included miniradiometers, GPS receivers, a mobile radiosonde system called the Mobile GPS Advanced Upper Air System (MGAUS), and shorter-wavelength radars (see Fig. 1). Geostationary Operational Environmental Satellite (GOES), mesonetworks of surface station data and National Weather Service (NWS) soundings fill out the suite of supplemental moisture information collected.

REFRACTIVITY PROCESSING FROM RESEARCH RADARS AND NEXRAD. The first successful experiments in retrieving radar refractivity measurements were made using the McGill University Doppler S-band radar in the 1990s. Subsequently, the radar refractivity technique was installed on the National Center for Atmospheric Research (NCAR) S-band dual-polarization Doppler radar (S-Pol) for collection of water vapor measurements in Oklahoma during the IHOP_2002 experiment. High correlations were observed between the S-Pol refractivity measurements and water vapor measurements obtained from IHOP-2002 surface stations, low-flying aircraft, profiling instruments, and radiosondes, lending credence that this refractivity technique can accurately estimate the water vapor in the lowest ~200–250 m AGL of the convective boundary layer (Weckwerth et al. 2005). Particularly exciting were measurements collected on the evolution of the Great Plains dryline and mesoscale outflow boundaries (Fabry 2006). IHOP_2002 also provided the opportunity to observe changes in refractivity (ΔN) associated with

REFRACTIVITY AND ITS MEASUREMENT BY RADAR

The refractive index n of a medium is defined as the ratio of the speed of light in a vacuum and the speed of light in that medium. In the atmosphere, near sea level, the refractive index n of air is typically around 1.0003, and its range of values rarely spans more than 100 ppm at any given location. For convenience, a derived quantity called the refractivity N is typically used, where $N = 10^6 (n - 1)$. For example, if $n = 1.000285$, subtracting 1 and multiplying by 10^6 will give $N = 285$. In the troposphere, N has been shown to depend on pressure (P), temperature (T), and water vapor pressure (e), by

$$N = N_{\text{dry}} + N_{\text{wet}} = 77.6\frac{P}{T} + 3.73\times10^{5}\frac{e}{T^{2}}, \qquad \text{(SB1)}$$

with pressures in hectopascals and temperature in kelvins (Bean and Dutton 1968). The first term proportional to air density is larger (225–325 N units), however most of the spatial variability in N results from the second term (0–150 N units). A change of 5 N units can be caused by a change of 5°C in temperature or of 1 hPa in vapor pressure, which corresponds to 1°C in dewpoint at room temperature. A 1°C change in dewpoint occurs more readily than a 5°C change in temperature, and thus fields of N can be seen qualitatively as proxies for fields of humidity during the summer. Quantitatively, given an average pressure and temperature over the radar coverage, humidity can be recovered with reasonable accuracy (Fabry and Creese 1999; Weckwerth et al. 2005).

As refractivity changes, so does the speed of light as well as the number of radar wavelengths between the radar and fixed ground targets (Fig. SB1). This slight change in the number of wavelengths between the radar and targets manifests itself by a change in the observed phase of these targets, which can be measured by the radar and then used to calculate refractivity. If enough fixed ground targets are present, which is often the case within 40 km of a radar, fields of refractivity can be obtained by radar with a spatial resolution on the order of a few kilometers (Fabry et al. 1997). Many atmospheric phenomena, whether associated with boundary layer processes or mesoscale or synoptic-scale events, are either caused by or result in gradients or variability in surface moisture. Through the refractivity measurement, these gradients can now be sampled and observed by radar.

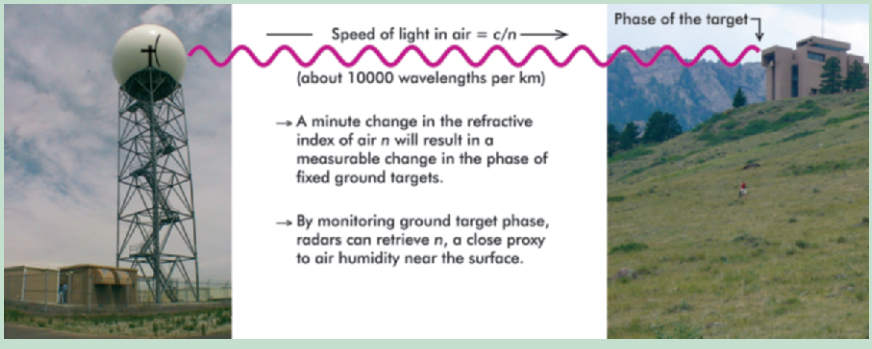

FIG. SB1. Illustration of the concept behind the measurement of the refractivity N of air near the surface by radar by using the returns from fixed ground targets.

atmospheric bores that traveled through Oklahoma (Koch et al. 2008).

Experience with S-Pol indicated that radar refractivity estimates could likely be obtained from other 10-cm-wavelength research radars and the operational NEXRAD. Realization of this stimulated the planning of a refractivity experiment (REFRACTT) that combined both research and operational radars in order to sample a larger area. It also meant that refractivity data collected from S-Pol could be used as an established gauge in comparing its measurements with those collected by the Denver NEXRAD (KFTG) radar and with the Colorado State University (CSU)–University of Chicago–Illinois State Water Survey (CHILL) radar in regions of overlapping measurements (see Fig. 1).

For REFRACTT, the CSU–CHILL and Pawnee research radars were modified to include the data collection and signal processing customizations required for refractivity measurements (see "Methodology for refractivity implementation" sidebar). The software run during IHOP_2002 for real-time calculation of radar refractivity on S-Pol was rewritten for REFRACTT to be more generic for any 10-cm-wavelength radar. A data processing protocol was established in which the raw archive format data obtained from the lowest radar elevation angle (0.0° from the research radars; 0.5° from the NEXRAD) were converted to netCDF format as soon as the radar elevation sweep was written to disk. This reformatted file was then transferred to NCAR using standard file transfer protocol (ftp) procedures, network, and T1 connections. By using these procedures, the available network bandwidth permitted the data reformatting and transmission steps to be completed within the 4-min volume scan cycle time. Thus, refractivity fields and refractivity mosaics were produced in real time every 4 min. Figure 2 illustrates the flow of data from the individual radars to computers at NCAR for production of the real-time mosaic refractivity fields and the display of all fields on a Web browser in the Denver NWS Weather Forecast Office (WFO).

Accessing the data from a completely operational NEXRAD system in 2006 presented many unique challenges and security issues, which were ultimately overcome. Retrieval of refractivity from the KFTG

METHODOLOGY FOR REFRACTIVITY IMPLEMENTATION

In principle, any Doppler weather radar can make the basic ground target measurements that are fundamental to the remote sensing of atmospheric refractivity. At every range sampling point (range gate), the received complex voltage signal, comprised of orthogonal components *I* and *Q*, are used to calculate the phase from each transmitted pulse. The radial velocity of a target is then estimated by averaging the pulse-to-pulse phase *change* over *M* consecutive pulses (~50–60 for typical antenna scan rates), but the individual *I* and *Q* values are not retained. In contrast, refractivity is measured by averaging the *I* and *Q* values for the same number of pulses to obtain a phase for that scan, and then calculating the phase *change* between two scans. Thus, the data stream from the radar must be modified to include the average *I* and *Q*, or alternatively the resulting phase, for each range gate. These average *I* and *Q* values must be generated prior to the standard "ground clutter" filtering, which is performed to suppress ground echoes from weather targets. Otherwise, the signals from ground targets, used to calculate refractivity, would be removed.

A calibration step is required to obtain *absolute* refractivity fields from radar data in real time (i.e., to associate the ground target phase observations to the atmospheric refractivity) by generating a reference phase field/scan. To accomplish this, phase values are averaged from data collected during a 10–30-min period of 1) spatially uniform refractivity as determined by surface station data and 2) limited temporal evolution as determined by the radar data itself. An *N* value based on the surface station data is then associated with this phase field to which real-time phase fields are compared to calculate the new refractivity value. The calibration of multiple radars located at different heights above sea level offered a special challenge because there is a modest dependency of refractivity on pressure. A common height was chosen and the pressure data were adjusted to that common level (Fabry and Creese 1999).

Refractivity change (ΔN) has also been shown to be meteorologically meaningful, highlighting moving fronts that are sometimes difficult to see on absolute refractivity maps. ΔN is calculated on a scan-to-scan basis and eliminates the need for the calibration scan. Given these advantages, both absolute refractivity and ΔN fields are estimated and used for further analysis.

A second important step is to collect data that will help in identifying reliable, nonmoving ground targets (see Fabry 2004). Power poles, transmission towers, and buildings make good targets; trees and lake surfaces are examples of poor targets because they are not temporally coherent.

A technical issue that had to be resolved was to verify the stability of the NEXRAD transmit frequency. To measure refractivity with a 1-*N*-unit accuracy, or the refractive index *n* with a 1 ppm accuracy, the stability of the radar transmit frequency must be within 1 ppm, a requirement that was not part of the original NEXRAD specifications. The transmit frequency was monitored during REFRACTT via a high-quality frequency counter and recorded using a PC. It was found that the frequency drift did not exceed 0.4 ppm.

radar required access to the radar time series information (level I data), which must be obtained directly from the RVP-8 processor. A firewall was installed (Fig. 2) that permitted only one-way data flow from the KFTG open radar data acquisition (ORDA) to NCAR. The final configuration was tested on the Radar Operations Center test bed Weather Surveillance Radar-1988 Doppler (WSR-88D; NEXRAD) radar in advance to ensure security requirements were met, perform interface certification testing, and verify necessary KFTG radar data acquisition (RDA) configuration changes.

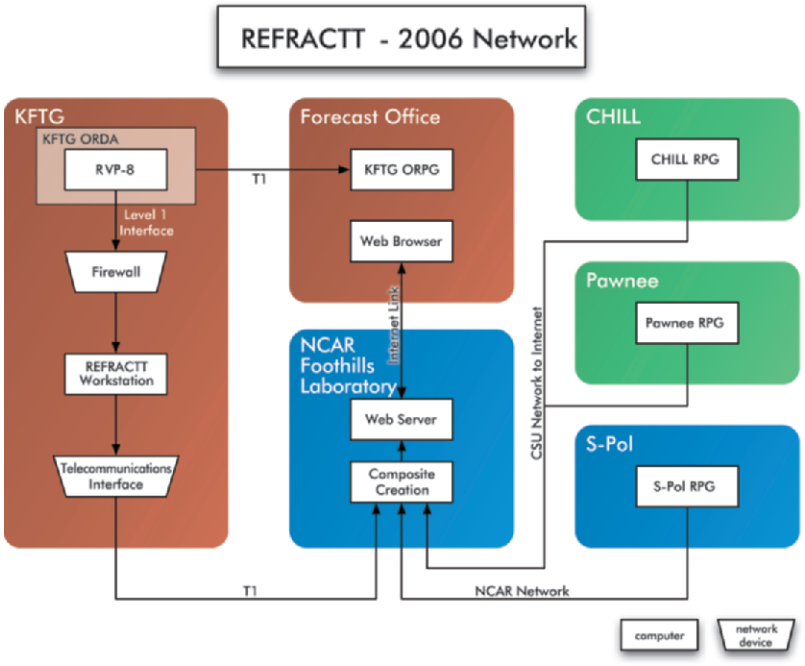

Fig. 2. Flowchart representing the processing and transfer of information from the four radar sites to NCAR and the Denver NWS WFO.

Figure 3 is an example of refractivity (N) fields from the S-Pol, CSU–CHILL, and KFTG radars at 0538 UTC 1 August 2006. Note the incredibly high-resolution (4-km grid spacing), detailed moisture information that can be obtained from the refractivity retrieval compared to the point measurements obtained from automated weather stations [Automated Surface Observing System (ASOS) and Automated Weather Observing System (AWOS)] that are overlaid. A change of 4 N units in the images corresponds to a change of ~1 g kg^{-1} of water vapor mixing ratio. Or conversely, a change of 5 N units (one color change in the N scale in Fig. 3) can be caused by a change of 5°C in temperature or 1°C in dewpoint at room temperature (see "Refractivity and its measurement by radar" sidebar). In Fig. 3, the individual radars all show an east–west moisture gradient, with lower moisture (N) values to the west and higher moisture values to the east. Combining the individual radar fields into a refractivity mosaic gives us a unique opportunity to see the broader picture, that is, the onset of a large-scale surge of higher moisture values that were moving into the Denver area from the eastern plains in the late evening, followed by the initiation of a line of intense thunderstorms. The mosaic image also highlights other subtleties in the water vapor field that are not directly evident from the individual radars and surface stations, including the N variability of 10–15 (2°–3°C in dewpoint temperature change), running north–south along the foothills of the Rocky Mountains and N change of 20 between S-Pol and CSU–CHILL radars.

HIGHLIGHTS OF REFRACTT 2006. There are many potential applications of a high-resolution, near-surface water vapor field. Examples of refractivity data collected during REFRACTT under a variety of scenarios are shown below highlighting some of these applications.

Monitoring boundary layer variability. One of the advantages of collecting near-surface water vapor information is the opportunity to examine its relationship to the underlying terrain. Figure 4 shows a common refractivity pattern observable on several days during REFRACTT prior to the start of convective activity. The 1650-m terrain contour is overlaid for geographical reference because it represents the beginning of the steep increase in terrain associated with the Rocky Mountains. It is worth noting that an appreciable amount of moisture retrieval was possible in the foothills of the Rocky Mountains. It is most intriguing, and perhaps not surprising, that the moisture field appears to have a broad pattern similar to the orientation of the network of rivers (and some dry creek beds) flowing through the Platte River Valley (see Fig. 1) and into the high-terrain areas. Indeed, the highest moisture pocket in the whole domain is centered over the CSU–CHILL radar site in the heart of the valley in a region of heavily irrigated fields. One can conceive of building a climatology of moisture patterns for particular geographic locations and correlating this

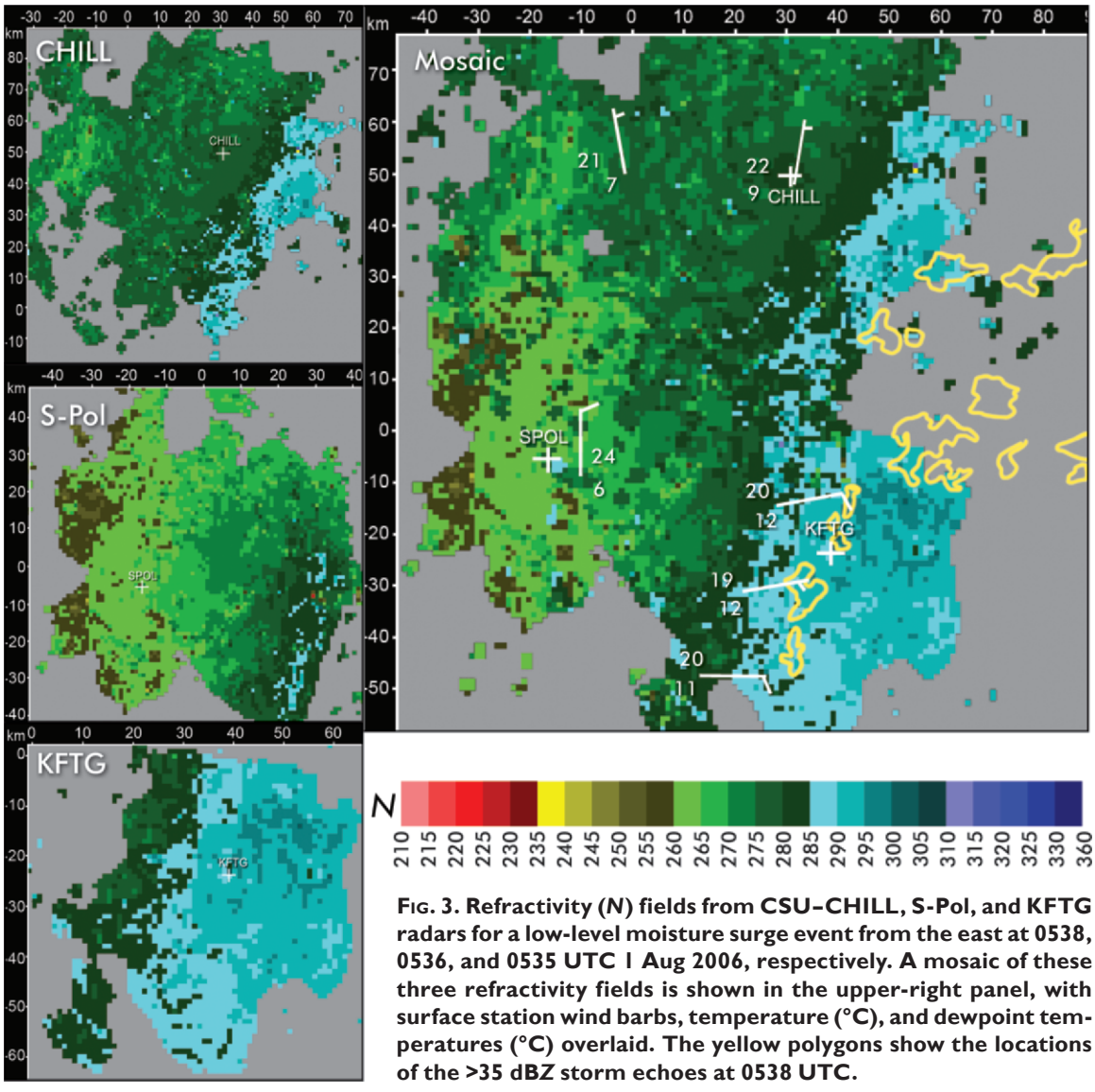

FIG. 3. Refractivity (*N*) fields from CSU–CHILL, S-Pol, and KFTG radars for a low-level moisture surge event from the east at 0538, 0536, and 0535 UTC 1 Aug 2006, respectively. A mosaic of these three refractivity fields is shown in the upper-right panel, with surface station wind barbs, temperature (°C), and dewpoint temperatures (°C) overlaid. The yellow polygons show the locations of the >35 dBZ storm echoes at 0538 UTC.

to the frequency of thunderstorm initiation. Fabry (2006) has used the IHOP_2002 refractivity data to build climatologies of moisture gradients versus time of day and prevailing wind direction.

Figure 5 represents the ~8-h evolution of the moisture field on 25 August collected by the KFTG NEXRAD radar. One of the most favorable scenarios for severe thunderstorm occurrence in northeast Colorado is the development of a Denver convergence and vorticity zone (DCVZ; Szoke et al. 1984), a terrain-induced, semistationary surface convergence feature that marks the boundary between moist southeasterly-to-northeasterly air and dry northwesterly air, and tends to be oriented roughly north–south through the Denver urban corridor. On this particular day, it was difficult to locate the exact position of the DCVZ on the radar reflectivity and Doppler velocity images; instead, a broad, highly variable convergence zone was discernible. In Fig. 5 the moisture gradient built up for several hours, arising either from moisture advection or surface evapotranspiration processes, prior to the convergence boundary becoming well defined at 1857 UTC in the reflectivity and velocity fields. Weckwerth et al. (2005) reported a very similar observation from IHOP_2002 where the radar refractivity field showed the development of the dryline in western Oklahoma well before it was observed as a radar thin line in reflectivity. Although clouds are observed to form above the DCVZ on satellite imagery beginning around 1800 UTC, other convective activity 20–30 km west of KFTG and environmental factors within the REFRACTT domain acted to shut off the convection directly over the DCVZ, and the moisture

gradient was observed to decrease thereafter. Detailed analyses remain to be conducted to understand where the moisture went.

Use of moisture fields by NWS forecasters. One of the objectives of REFRACTT was to provide the NWS forecasters with refractivity data and receive feedback on its utility for short-term forecasting. Training on refractivity data was provided to the WFO Denver/Boulder (BOU) staff as part of their convective season workshop. Forecasters accessed the information via the Internet on PCs adjacent to the workstations used for forecast and warning decisions. The Web site functioned well and forecasters were pleased with the capability to view rapidly updating, high-resolution moisture fields in real time. However, recurring data communications problems via the Web browser, delays in getting security clearance for the KFTG data access, and the rendering of refractivity fields on a display external to their Advanced Weather Interactive Processing System (AWIPS) workstation limited the forecasters' use of the data. Nonetheless, some favorable comments from forecasters are presented below.

One of the challenges the forecasters face in the summertime is knowing when higher moisture will be moving back into the Platte River Valley and the Denver area from the northeast (see Fig. 1), a precursor to active thunderstorm development later in the day. One of the Denver forecasters described using the refractivity field as part of a family of analytical tools to track the gradual increase in postfrontal moisture across northeast Colorado late in the afternoon and evening of 31 July–1 August (Fig. 3). He found the field particularly useful in monitoring the formation and movement of a strong north–south convergence boundary in eastern Colorado coinciding with

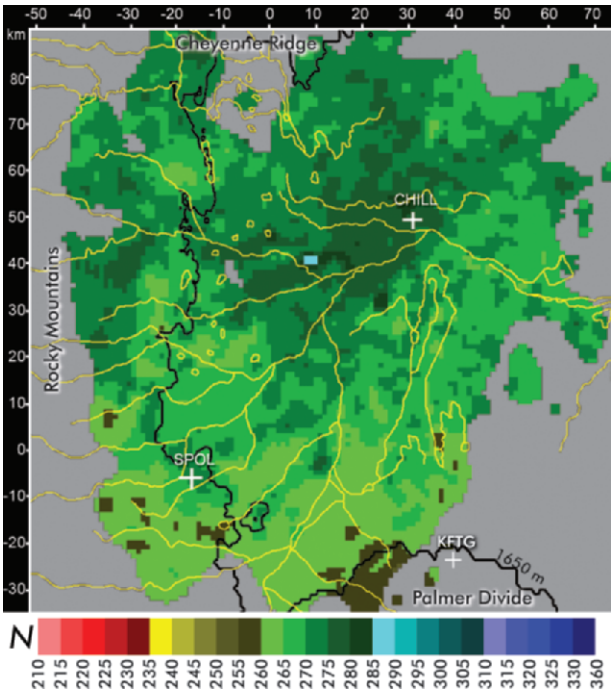

Fig. 4. S-Pol and CSU–CHILL refractivity mosaic at 2006 UTC 25 Jul 2006. The network of rivers in northeast Colorado are overlaid onto the refractivity field, along with a contour of the terrain at 1,650 m.

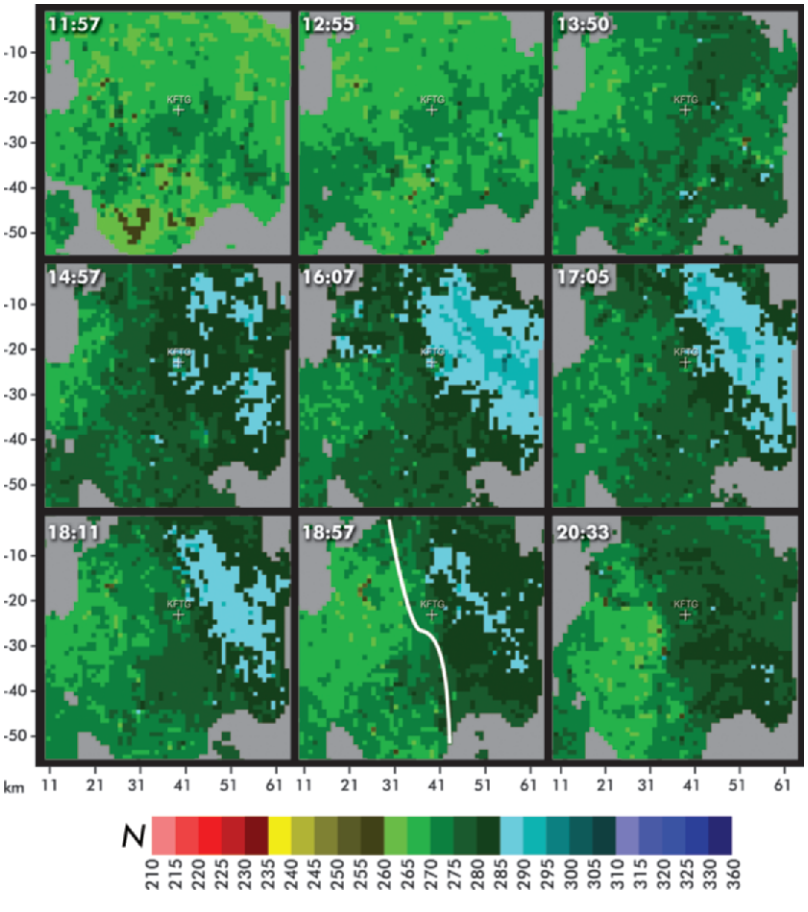

Fig. 5. Time series of refractivity images of the development of the Denver convergence/vorticity zone (DCVZ) as observed by the Denver KFTG NEXRAD radar on 25 Aug 2006. The location of the DCVZ (solid white contour) is shown at 1857 UTC based on radar reflectivity and velocity information.

the location of the highest N values (285–290). This north–south boundary eventually triggered a line of intense storms that produced heavy rain, localized flooding, hail, and lightning.

Tracking cold frontal passage. After REFRACTT had formally ended, the KFTG refractivity collections continued for the Denver WFO until December. On 11 October 2006, a cold front approached Denver from the northeast. Frontal passage was characterized by a decrease in surface station temperature of over 2°C, an increase in surface mixing ratio of nearly 1 g kg^{-1}, and an increase in surface wind speeds from the northeast. Figure 6 shows that the leading edge of the postfrontal airmass is clearly demarcated in the ΔN field, the difference between the two most recent N retrievals, and in the band of high (blue) ΔN values. The forecasters commented that the refractivity data did an outstanding job of identifying the movement of a frontal passage across the Denver area. They felt the resolution of the front was much more detailed than the information provided by radar fine lines and surface data.

Mesoscale predictability of convection. On 20 July 2006 widespread convection broke out in the REFRACTT domain as illustrated in the series of radar reflectivity images in Fig. 7. Storms initially formed over the higher terrain of the Rocky Mountains, and later storms were triggered over the plains by a thunderstorm outflow (Figs. 7d,g) from the south. A northwest–southeast gradient of moisture was present throughout the day with higher moisture located along the foothills and over the Platte River Valley. Smaller (spatial)-scale moisture gradients were also evident, associated with the gust front (Fig. 7e), and a semistationary convergence feature was barely evident in the reflectivity field (Figs. 7a,d,g) but was noted in the refractivity field (Figs. 7b,e,h). Computing the change in the moisture values over hourly intervals (Figs. 7c,f,i) provides a quick snapshot of changes occurring in the prestorm and storm environments. At 2018 UTC, we see that only small changes in moisture had been occurring throughout the domain. At 2118 UTC, large increases in N are observed following gust front passage. Of particular interest, at 2210 UTC, is the increase in moisture observed within the past hour along the semistationary convergence feature. The increasing moisture convergence in this region preceded the development of thunderstorms within the next half-hour (Fig. 7g).

A key factor in predicting atmospheric convection is the observation that sufficient moisture is available not just at the surface, but through the boundary layer depth to support storm development. Thus, a pressing concern in the use of refractivity fields is having an understanding of both the environmental scenarios and the frequency of occurrence in which the near-surface refractivity moisture measurements typify the moisture profile through the depth of the boundary layer. Eighty MGAUS soundings were launched during REFRACTT specifically to enable comparisons of the 2D refractivity fields with vertical profiles of moisture. The vertical moisture profiles from two MGAUS soundings at 1906 and 2212 UTC (Fig. 8) are compared with the refractivity measurements at the corresponding times and locations shown in Fig. 7. There is good agreement between the near-surface mixing ratio values calculated from N and that measured by the sounding (see Fig. 8). In this particular case (although not for all cases), the surface refractivity values also reflect the moisture measured throughout the boundary layer depth. The 1902 UTC sounding illustrates the higher moisture that is present in the northwest portion of the REFRACTT domain, a boundary layer depth of ~1.3 km, and the substantial convective inhibition in the environment. Storms were able to form only over the mountains (Fig. 7a). By 2212 UTC, the depth of the boundary

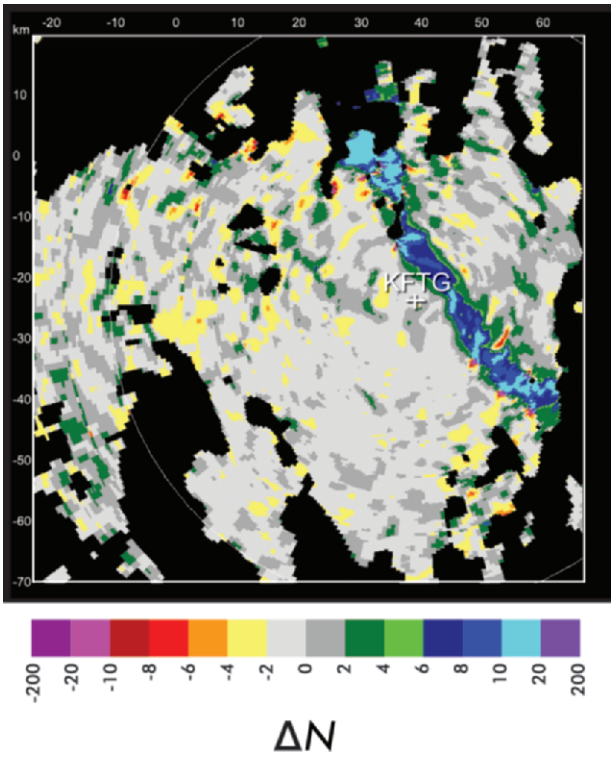

Fig. 6. Cold front approaching Denver at 1907 UTC 11 Oct 2006, as observed in the KFTG NEXRAD ΔN field computed over the previous 4-min period.

layer almost doubled during the intervening time period, and although the N and sounding moisture values are approximately 3 g kg^{-1} lower, convective inhibition was much less and storms formed quickly above surface convergence and moisture gradients.

In contrast, 9 August 2006 began with reasonably high surface moisture (Fig. 9a), although not quite as high as on 20 July. Once the shallow morning inversion shown in Fig. 9e at 1200 UTC was mixed out modest convective available potential energy was

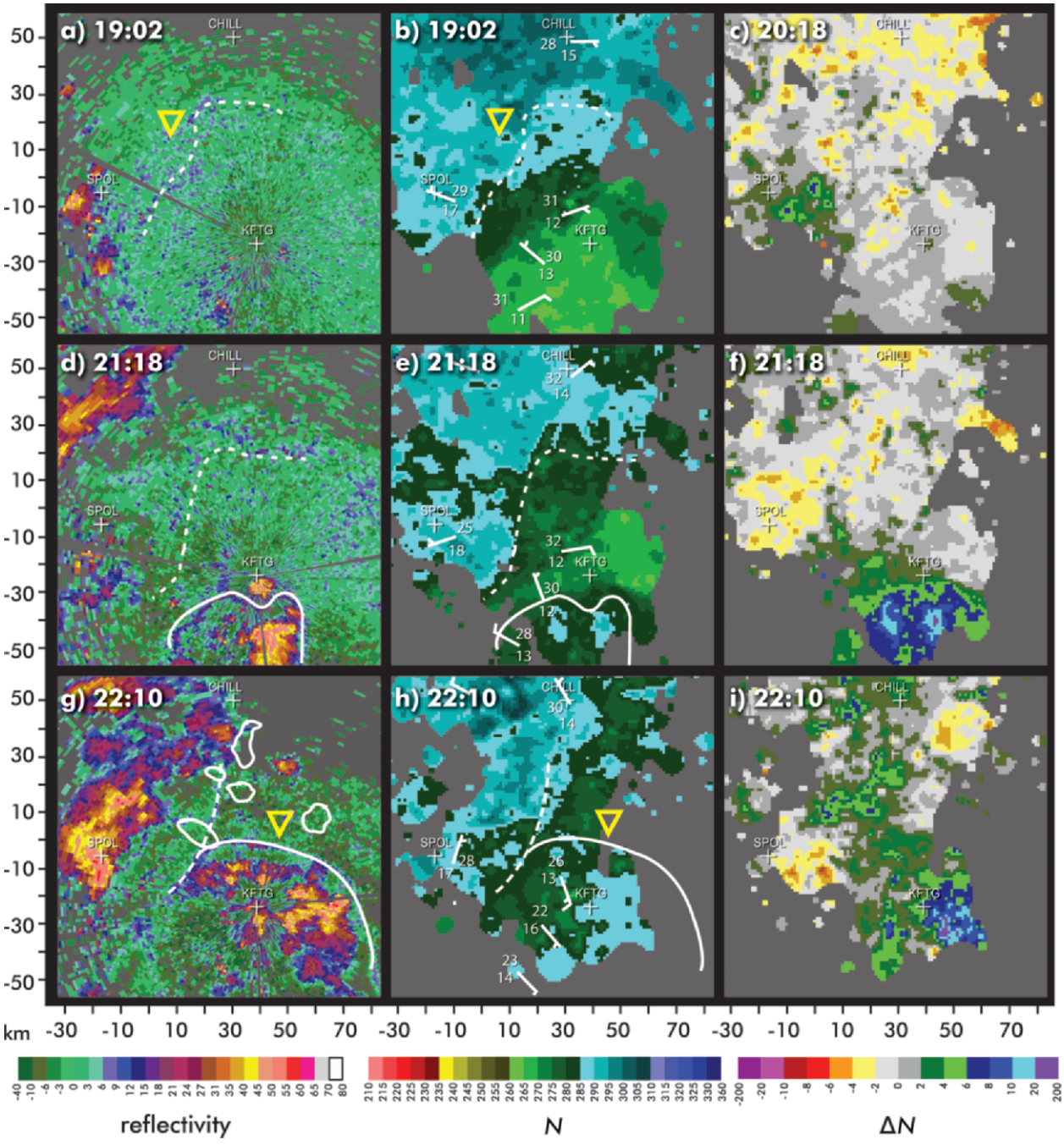

Fig. 7. Time series of radar reflectivity, mosaic refractivity, and Δ*N* plots on 20 Jul 2006 as thunderstorms develop over the plains. Solid white lines represent the locations of a gust front and dashed white lines show the location of a weak stationary convergence line. Yellow triangles show the location of the MGAUS soundings plotted in Fig. 8. The white polygons in (g) indicate the new storm locations observed by the radar at 2230 UTC. (a), (d), and (g) Reflectivity fields at 1902, 2118, and 2210 UTC, respectively; (b), (e), and (h) mosaics of refractivity data from CSU–CHILL, S-Pol, and KFTG at 1902, 2118, and 2210 UTC, respectively; and (c), (f), and (i) hourly Δ*N* images computed over the previous 60 min ending at 2018, 2118, and 2110 UTC, respectively.

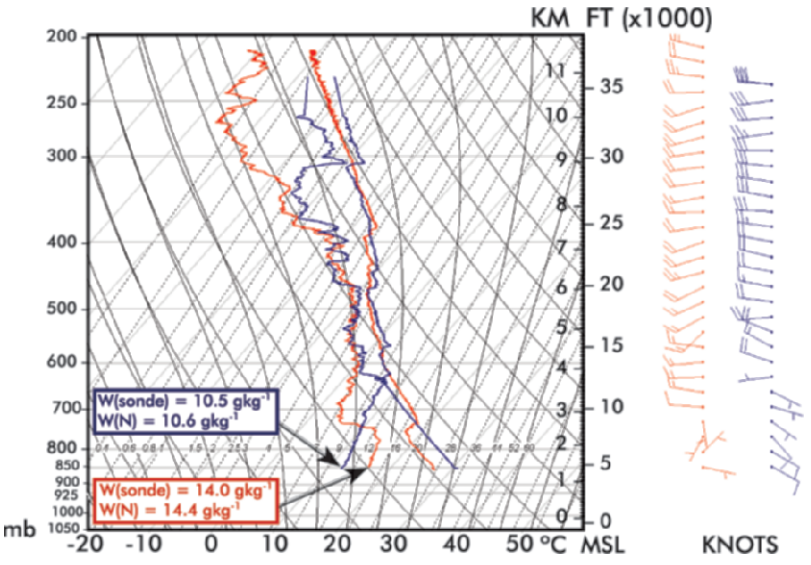

FIG. 8. MGAUS soundings showing boundary layer moisture variability during the development of thunderstorms at (a) 1906 (red profile) and (b) 2212 UTC (blue profile) 20 Jul 2006. Mixing ratio values measured in the lowest 25 hPa of the soundings *w(sonde)* and calculated from the *N* values *w(N)* at the sounding launch locations are shown. Location of sounding launches are shown in Fig. 7.

available, resulting in the chance for isolated thunderstorms. While monitoring the refractivity field in real time, a wedge of drier moisture values appeared west of the CSU–CHILL radar (Fig. 9b). Because of its unusual shape and rather sudden appearance, it was believed to be an artifact in the refractivity processing. Remarkably, it was actually the start of rapid drying that subsequently occurred throughout the REFRACTT domain over the next 2 h (Fig. 9d). Refractivity values plummeted by 60 *N* units; dewpoint temperatures recorded by the surface weather stations showed a drop of 11°C in the same time period. The MGAUS sounding taken at 1826 UTC shows that significant drying occurred through the depth of the boundary layer, negating the chance for thunderstorms.

Cursory examination of other cases highlights the necessity in tracking moisture changes in concert with the movement of the boundary layer winds and vertical profiles of moisture for improved understanding of convection initiation processes and storm predictability. Research into correlations of refractivity fields with MGAUS vertical moisture profiles, boundary layer wind observations, and convective initiation are ongoing.

ON THE HORIZON. *Assimilation of refractivity into NWP models.* The inherent difficulty of predicting initial storm development in mesoscale numerical models has been partially attributed to the lack of information about high-resolution moisture distribution (Sun and Crook 1997; Dowell et al. 2004; Sun 2005a,b). The radar refractivity observation provides a unique dataset that, when assimilated along with the radar radial velocity and reflectivity, can enhance low-level moisture analysis, and hence has the potential to improve the prediction of convective initiation. A preliminary data assimilation study using refractivity data collected by S-Pol during IHOP_2002 was reported in Sun (2005b). In that study, an experiment with refractivity, radial velocity, and reflectivity data assimilation was compared with one that only assimilates radial velocity and reflectivity. The study showed that the inclusion of refractivity data increased the water vapor variability, resulting in an improved forecast of storm initiation, precipitation intensity, and spatial extent. However, during IHOP_2002, refractivity data were produced from only the S-Pol radar. REFRACTT 2006 provides refractivity observations from four radar. This larger domain of moisture information makes it a unique dataset to study the impact of radar refractivity observations on data assimilation and numerical prediction of storm initiation and evolution.

Currently efforts are underway to assimilate REFRACTT observations for the convective event that occurred during the evening of 31 July–1 August (see Fig. 3) using the Variational Doppler Radar Analysis System (VDRAS; Sun and Crook 1997). VDRAS is a four-dimensional variational data assimilation (4DVAR) radar system that has been used both in research and in field operations. It provides a unique way to combine the refractivity observation with mesoscale model analysis, surface observation, and radar winds to produce a comprehensive analysis. Specific challenges will need to be addressed, including the fact that refractivity observations are limited in both the horizontal and vertical dimensions.

Producing 3D moisture fields. The radar refractivity technique only provides estimates of water vapor near the surface. To obtain 3D profiles of water vapor throughout the depth of the boundary layer, the refractivity fields will be combined

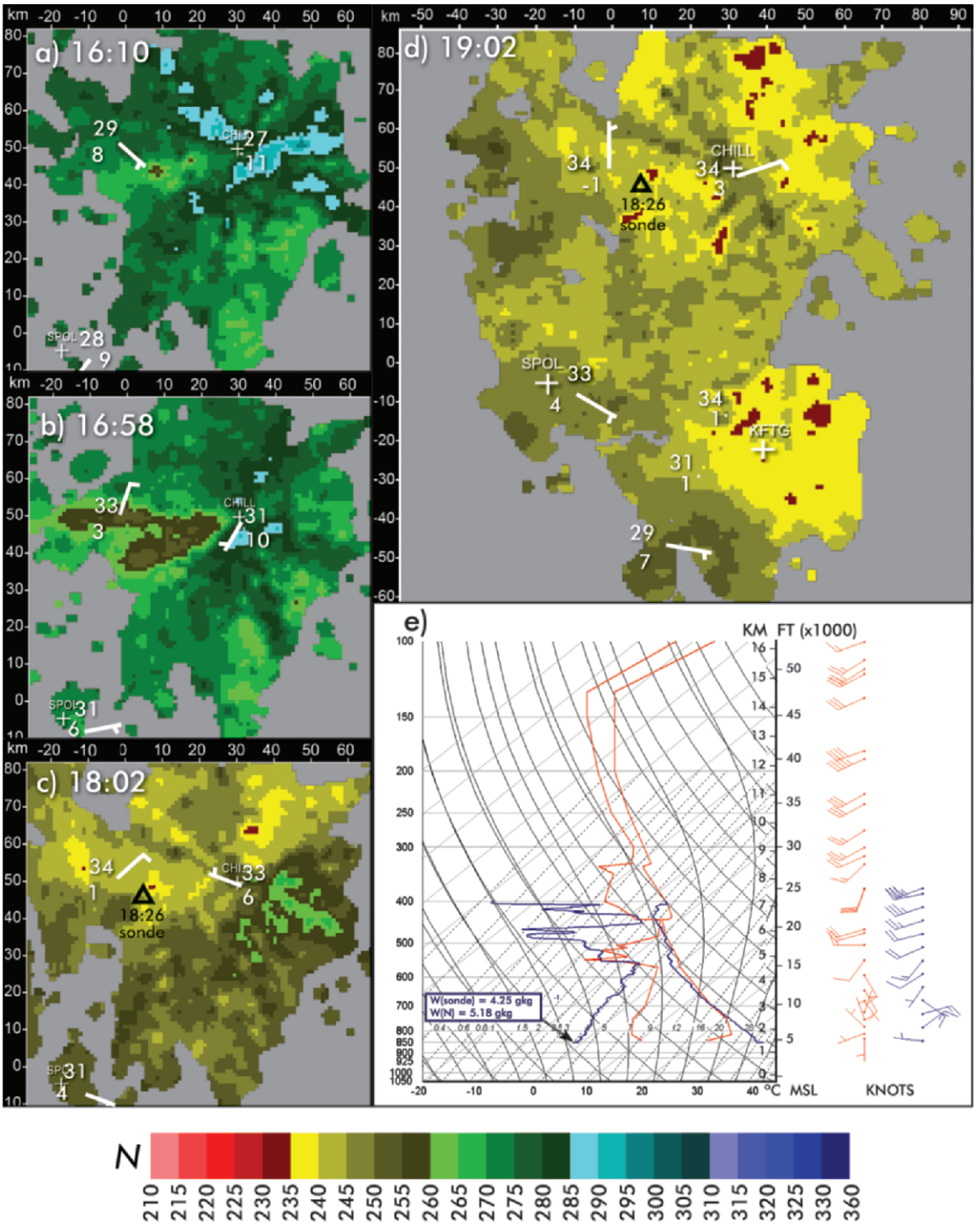

Fig. 9. Refractivity images and sounding profiles for a rapid boundary layer drying event on 9 Aug 2006. (a)–(c) Refractivity images from CSU–CHILL radar at 1610, 1658, and 1802 UTC, respectively. Surface station information are overlaid; (d) mosaic of refractivity from the CSU–CHILL, S-Pol, and KFTG radars at 1902 UTC with surface station information overlaid; (e) MGAUS sounding (blue) at 1826 UTC plotted with the NWS 1200 UTC sounding (red). The location of the MGAUS launch is shown in (c) and (d). Mixing ratio value measured by the MGAUS sounding *w(sonde)* and calculated from the *N* value *w(N)* at the sounding launch location is shown.

with vertical profiles of water vapor retrieved from other remote sensing platforms deployed during REFRACTT.

Twenty-one GPS stations were used during the REFRACTT operational season (see Fig. 1). This network was a composite of networks operated by the

University Corporation for Atmospheric Research (UCAR), National Oceanic and Atmospheric Administration (NOAA), SuomiNet (Ware et al. 2000), a private network of stations, and three temporary stations. GPS estimates of precipitable water vapor (PW; Bengsson et al. 2003) and line-of-sight slant water vapor (SWV; Braun et al. 2001, 2003) are complementary observations to surface refractivity measurements. A detailed study of the relationship between GPS SWV and radar refractivity observations is planned. The focus of the study will be to quantify the differences in the moisture fields to help identify when low-level convergence penetrates through the boundary layer leading to convection initiation.

The S-Pol includes simultaneous and coincident dual-wavelength (10 and 0.8 cm) radar measurements (Farquharson et al. 2005). By using the differential attenuation properties of the dual-wavelength radar observations, it is possible to retrieve the following two important meteorological quantities: vertical profiles of humidity outside the clouds, and liquid water content (LWC) within the clouds. The humidity profiles have been shown to be accurate to within about ±0.75 g m^{-3} (Ellis and Vivekanandan 2006). A major goal of the dual-wavelength radar work during REFRACTT was to combine the dual-wavelength humidity profiles with the near-surface refractivity retrievals to obtain a three-dimensional humidity field from the radar platform, an unprecedented measurement. The usefulness of the dual-wavelength humidity profiles and cloud LWC retrievals to improve numerical weather forecasts will be investigated by assimilating these data into a numerical weather prediction model.

The compact microwave radiometer for humidity profiling (CMR-H) was deployed (see Fig. 1) side by side with the commercially available Radiometrics WVP-1500 water vapor and liquid profiler radiometer. The CMR-H measures sky brightness temperatures simultaneously at four frequencies that are chosen for maximum water vapor information content (i.e., 22.12, 22.67, 23.25, and 24.50 GHz; Iturbide-Sanchez et al. 2007). The CMR-H is the first microwave radiometer specifically designed to operate as a node in a coordinated ground-based network for atmospheric observations. In such a network, multiple CMR-H nodes provide different perspectives on the same volume of the atmosphere, enabling tomographic inversion to retrieve the 3D tropospheric water vapor field. Improved measurement of the 3D water vapor field and their assimilation into numerical weather prediction models may improve weather forecasting, in particular the location and timing of the initiation of intense convective activity, including those causing tornadoes and flash floods.

Use of shorter-wavelength radars. As a consequence of REFRACTT 2006, subsequent studies have been started to determine whether refractivity retrieval methods can be run on shorter-wavelength radars. During REFRACTT, the University of Massachusetts 3-cm wavelength [X-band dual-polarization Doppler radar (X-Pol)] Adaptive Sensing of the Atmosphere (CASA)-like radar, operated by the University of Oklahoma, was collocated with the CSU–CHILL radar (see Fig. 1) for collection and intercomparison of refractivity fields. The results, while initially promising, need further examination. More extensive experiments are currently being carried out with the CASA X-band radar network in Oklahoma.

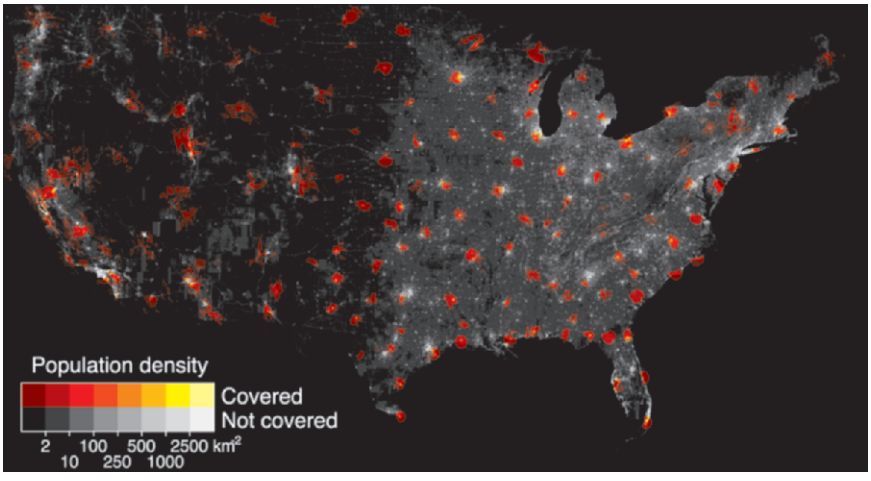

Fig. 10. Population density of the conterminous United States that would be under (yellow–red color scale) and outside (grayscale) refractivity coverage if the refractivity technique would be implemented on the NEXRAD (WSR-88D) radars. Although the coverage is limited, it incorporates more than 15% of the population.

Path to operations. REFRACTT 2006 provided a unique and timely opportunity to test the retrieval of refractivity from the new RVP-8 NEXRAD radar processor that is part of the ORDA system installed on

the NEXRAD radars in 2006. The infrastructure of the ORDA system facilitated access to the raw radar phase information required to run this technique in real time. The examples presented here from the NEXRAD radar highlight the very high-resolution moisture measurements that can now be obtained from an existing operational system. The next step is to define the path for implementation of the refractivity technique on the national network of radars for access by both the research and forecast community.

Figure 10 shows the anticipated spatial coverage of refractivity measurement from the NEXRAD over the continental United States overlaid on a population density map. While the coverage is seemingly sparse, it tends to be concentrated on either urban or suburban areas, the very same areas for which the NWS forecasters are under the greatest pressure to produce accurate and timely convective storm outlooks and short-term thunderstorm forecasts. It is evident from Fig. 10 that relying solely on NEXRAD collection of moisture leaves large gaps in the coverage. It will therefore be of great importance to extend the coverage by including refractivity measurements from the Federal Aviation Administration (FAA) radars, such as the national network of 5-cm-wavelength terminal Doppler weather radars. Of particular interest for the aviation community is the detection of those thunderstorm outflows in the terminal airport environment that are not initially observed in the radar reflectivity and velocity fields, but are evident early in the refractivity field as moisture gradients (M. Weber 2005, personal communication). Supplemental refractivity coverage could be provided by the CASA radar networks as well given the relatively close spacing of approximately 30 km.

In addition to the United States and Canada, several other countries are conducting feasibility studies on the collection of refractivity data from their operational weather radars. The Met Office and the University of Reading are well on their way to installing refractivity on their operational network of 5-cm-wavelength radars (J. Nichol 2006, personal communication). Australia and Taiwan will be installing the refractivity software on research radars for collecting during their convective weather seasons in 2007 and 2008.

The ability to use existing radars for totally new and desired applications really captures the imagination. In this paper, we have highlighted just a few of the potential uses of this field for variety of applications. The near-term challenge will be to combine these 2D measurements with vertical profiles of water vapor retrieved from other remote sensors to produce the high-resolution 3D moisture observations. Refractivity retrieval from radar is the first promising step in obtaining the high-resolution water vapor measurements needed to predict the precise location and timing of convection initiation and produce accurate quantitative precipitation forecasts.

ACKNOWLEDGMENTS. We greatly appreciate the high level of support from the S-Pol and CSU–CHILL radar and software engineers and technicians, particularly Mike Dixon, Dave Brunkow, John Hubbert, Al Phinney, Jim George, Robert Bowie, Dennis Flanigan, Gordon Farquharson, and Dean Lauritsen. Jeff Cole's assistance was invaluable in getting the MGAUS system built. We are especially grateful to Jonathan Emmett, Kyle Holden, Brian Pereira, Mike Strong, and Laura Tudor who did double duty supporting both the S-Pol operations and running the MGAUS system. Boon Leng Cheong, Kery Hardwick, Pei-Sang Tsai, and Stephen Frasier fulfilled the last-minute request of getting the X-Pol radar to Colorado and provided dedicated support. Lara Ziady did a phenomenal job finalizing the figures. ShinJu Park provided an early review of the manuscript. Raja Sengupta produced an earlier version of Fig. 10. We wish to acknowledge the tremendous efforts of Christina Horvat, John Heimer, Rex Reed, and Joe Muffoletto at the Radar Operations Center in Norman in getting triagency approval to access the KFTG ORDA data. We are particularly grateful to Stephan Nelson and James Huning, who on behalf of the National Science Foundation, made REFRACTT 2006 possible.

REFERENCES

Bean, B. R., and E. J. Dutton, 1968: *Radio Meteorology.* Dover Publications, 435 pp.

Bengsson, L., and Coauthors, 2003: The use of GPS measurements for water vapor determination. *Bull. Amer. Meteor. Soc.,* **84,** 1249–1258.

Braun, J. J., C. Rocken, and R. H. Ware, 2001: Validation of single slant water vapor measurements with GPS. *Radio Sci.,* **36,** 459–472.

——, ——, and J. Liljegren, 2003: Comparisons of line-of-sight water vapor observations using the global positioning system and a pointing microwave radiometer. *J. Atmos. Oceanic Technol.,* **20,** 606–612.

Crook, N. A., 1996: Sensitivity of moist convection forced by boundary layer processes to low-level thermodynamic fields. *Mon. Wea. Rev.,* **124,** 1767–1785.

Dabberdt, W. F., and T. W. Schlatter, 1996: Research opportunities from emerging atmospheric observing and modeling capabilities. *Mon. Wea. Rev.,* **124,** 1767–1785.

Dowell, D. C., F. Zhang, L. J. Wicker, C. Snyder, and N. A. Crook, 2004: Wind and temperature retrievals in the 17 May 1981 Arcadia, Oklahoma, supercell: Ensemble Kalman filter experiments. *Mon. Wea. Rev.,* **132,** 1982–2005.

Ellis, S. M., and J. Vivekanandan, 2006: Water vapor and liquid water estimates using simultaneous S and Ka-band radar measurements. *Proc. Fourth European Conf. on Radar Meteorology and Hydrology,* Barcelona, Spain, ERAD, 240–243.

Emanuel, K., and Coauthors, 1995: Report of the first prospectus development team of the U.S. weather research program to NOAA and the NSF. *Bull. Amer. Meteor. Soc.,* **76,** 1194–1208.

Fabry, F., 2004: Meteorological value of ground target measurements by radar. *J. Atmos. Oceanic Technol.,* **21,** 560–573.

——, 2006: The spatial structure of moisture near the surface: Project-long characterization. *Mon. Wea. Rev.,* **134,** 79–91.

——, and C. Creese, 1999: If fine lines fail, try ground targets. Preprints, *29th Int. Conf. on Radar Meteorology,* Montreal QC, Canada, Amer. Meteor. Soc., 21–23.

——, C. Frush, I. Zawadzki, and A. Kilambi, 1997: On the extraction of near-surface index of refraction using radar phase measurements from ground targets. *J. Atmos. Oceanic Technol.,* **14,** 978–987.

Farquharson, G., and Coauthors, 2005: NCAR S-Pol second frequency (Ka-band) radar. Preprints, *32nd Conf. on Radar Meteorology,* Albuquerque, NM, Amer. Meteor. Soc., P12R.6. [Available online at http://ams.confex.com/ams/pdfpapers/97141.pdf.]

Iturbide-Sanchez, F., S. C. Reising, and S. Padmanabhan, 2007: A miniaturized spectrometer radiometer based on MMIC technology for tropospheric water vapor profiling, *IEEE Trans. Geosci. Remote Sens.,* **45,** 2181–2194.

Koch, S. E., W. Feltz, F. Fabry, M. Pagowski, B. Geerts, K. Bedka, D. Miller, and J. Wilson, 2008: Turbulent mixing processes in atmospheric bores and solitary waves deduced from profiling systems and numerical simulation. *Mon. Wea. Rev.,* **136,** 1373–1400.

National Research Council, 1998: *The Atmospheric Sciences: Entering the Twenty-First Century.* National Research Academy Press, 364 pp.

Sun, J., 2005a: Initialization and numerical forecasting of a supercell storm observed during STEPS. *Mon. Wea. Rev.,* **133,** 793–813.

——, 2005b: Convective-scale assimilation of radar data: Progress and challenges. *Quart. J. Roy. Meteor. Soc.,* **131,** 3439–3463.

——, and N. A. Crook, 1997: Dynamical and microphysical retrieval from Doppler radar observations using a cloud model and its adjoint. Part I. Model development and simulated data experiments. *J. Atmos. Sci.,* **54,** 1642–1661.

Szoke, E. J., M. L. Weisman, J. M. Brown, F. Caracena, and T. W. Schlatter, 1984: A subsynoptic analysis of the Denver tornadoes of 3 June 1981. *Mon. Wea. Rev.,* **112,** 790–808.

Ware, R. H., and Coauthors, 2000: SuomiNet: A real-time national GPS network for atmospheric research and education. *Bull. Amer. Meteor. Soc.,* **81,** 677–694.

Weckwerth, T. M., and Coauthors, 2004: An overview of the International H_2O Project (IHOP_2002) and some preliminary highlights. *Bull. Amer. Meteor. Soc.,* **85,** 253–277.

——, C. R. Pettet, F. Fabry, S. Park, J. W. Wilson, and M. A. LeMone, 2005: Radar refractivity retrieval: Validation and application to short-term forecasting. *J. Appl. Meteor.,* **44,** 285–300.